



Hybrid Solder Joint for Low-Temperature Bonding Application

Yu-Yuan Lai¹ · Jui-Lin Chao¹ · Chia-Jung Hsu¹ · Chang-Meng Wang² · Albert T. Wu¹

Received: 12 September 2022 / Accepted: 17 November 2022 / Published online: 8 December 2022
© The Minerals, Metals & Materials Society 2022

Abstract

Low-temperature bonding has become a significant trend in advanced electronics packaging technology. A low-reflow-temperature process can effectively reduce the risk of warpage, thus greatly enhancing device reliability. SnBi eutectic solder is one of the best candidates for low-temperature assembly. In this study, first, a layer of pre-solder (Sn-0.3Ag-0.7 Cu, SAC0307) was reflowed; then, another layer of low-temperature solder (Sn-56Bi-1Ag-0.2Cu, SB102) was reflowed on top to create a hybrid solder joint. Small bismuth precipitates were uniformly distributed in the SAC0307 layer after long-term aging. Cross-sectional images were examined to analyze the kinetics between the SB102/SAC interdiffusion reaction. Shear tests and fracture surface analyses were undertaken to investigate the joint strength and the failure mode. The SAC0307 layer prevented the solder embrittlement by reducing the ratio of Bi-rich phases in the SB102 matrix and successfully transformed the mechanical fracture mode from brittle to ductile. The results demonstrated that the mechanical properties of the solder joint were greatly improved after long-term heat treatment.

Keywords SAC0307 · hybrid solder joint · SnBi · low-temperature

Introduction

As the miniaturization trend of large-scale-circuit integration is approaching the limit of Moore's law, the electronics industry has been searching for ways to overcome or extend the limit of Moore's law. One promising method is the assembly of a three-dimensional integrated circuit (3D IC). Package-on-package is a common 3D IC method, wherein the role of solder joints is critical when stacking two different components on the same package. However, the reflow of traditional SAC305 Pb-free solder requires a reflow temperature of around 250°C. Such a high temperature induces thermal stress between the Si chips and polymer substrates due to the difference in their thermal expansion coefficients. Furthermore, the thermal stress may induce severe warpage, thus damaging the chips.

Compared with other common Pb-free solders used in the industry, Sn-58Bi (SnBi) alloy has a relatively low melting point (139°C) with good wettability and high mechanical

strength.^{1–5} Despite being a promising low-temperature solder, however, a continuous Bi-rich phase can disintegrate, and an intermetallic compound (IMC) layer formed at the interface between the Sn-Bi solder matrix and the substrate significantly reduces the joint strength after long-term heat treatment.¹ When the composition of SnBi was modified by alloying a minor amount of Ag, a continuous brittle Bi-rich layer was not observed for the entire aging process.² With the addition of Ag, the increased apparent activation energy inhibits the high growth rate of IMC.³ Although the mechanical properties of SnBiAg were enhanced by the addition of minor Ag, the morphology of the fracture surface still exhibited brittle behavior.⁴ For advanced electronics packaging technology, the solder joints should have sufficient strength and ductility as well as high reliability. Furthermore, it is essential to prevent the formation of cracks between the solder joints and Cu wires.⁵

In our research, SnBi with minimal alloying with Ag and Cu was chosen as the low-temperature bonding material, exhibiting a low melting point and superior mechanical properties. The alloy is expected to reduce the risk of thermal warpage and enhance the device reliability after long-term aging. To fulfill the demand for high ductility in 3D IC, the hybrid solder joint contained Sn-56Bi-1Ag-0.2Cu (SB102) on top and Sn-0.7Ag-0.3Cu (SAC0307) on

✉ Albert T. Wu
atwu@ncu.edu.tw

¹ Department of Chemical and Materials Engineering, National Central University, Taoyuan City 32001, Taiwan

² Shenmao Technology INC, Taoyuan City 32841, Taiwan

the bottom, and the reflow temperatures were set as 170°C and 190°C. By utilizing the ductile SAC solder after reflow and long-term aging,^{6,7} the hybrid solder joint exhibited improved ductility by reducing the ratio of Bi-rich phases. The mechanical properties could be enhanced by an interdiffusion between SB102 and SAC0307 post-heat treatment. The hybrid solder joint microstructure was observed after reflowing at 170°C and 190°C via a scanning electron microscope and a backscattered electron microscope. To verify the relationship between the Sn dissolution rate at different reflow temperatures, a liquid/solid interdiffusion reaction test was conducted by immersing an SAC solder wire in molten SB102 solder. The mechanical properties of the hybrid solder joint were investigated by a shear test that involved analyzing the fracture surface and the shear strength after long-term aging.

Experimental Methods

The hybrid solder joint used in this study was provided by Shenmao Technology Inc. An Sn–0.3Ag–0.7Cu (SAC0307) solder paste was screen-printed on a predefined Cu pad on a printed circuit board (PCB), followed by the reflow. An Sn–56Bi–1Ag–0.2Cu (SB102) solder paste was then screen-printed above the reflowed SAC0307 solder cap, followed by another reflow at 170°C and 190°C. The reflow dwell time at peak temperature (170°C) was 75 s. The heating rate and cooling rate were 1.45°C/s and –0.9°C/s, respectively. Another reflowed time dwelled at peak temperature (190°C) for 75 s, and the heating rate and cooling rate were 1.75°C/s and –1.25°C/s, respectively. Samples with only SB102 screen-printed and reflowed on PCB were fabricated for comparison. All the samples were sealed in vacuumized glass tubes to minimize oxidation interference after the long-term reliability test. The samples were aged at 100°C for 15 days. Subsequently, the samples were mounted in epoxy and carefully ground and polished to reveal the desired cross-section. The cross-sectional images and phase compositions were analyzed by scanning electron microscope (SEM, S-300H, Hitachi) in a backscattered electron (BSE) imaging mode and an electron dispersive spectrometer (model 7582, Oxford Instruments), respectively. Shear test samples were aged at 75°C, 100°C, and 125°C for 15 days. To confirm the relationship between the reflow temperature and the dissolution rate of Sn in SB102, an SAC305 wire was immersed in the molten SB102 solder bath at 140°C, 150°C, and 160°C for different intervals. 25 g of SB102 solder paste was first melted in a Petri dish and heated to 140, 150, and 160°C. The temperature of the liquid SB102 was monitored by inserting a K-type thermocouple into the liquid SB102. Five-centimeter SAC305 wires with an average diameter of 845 µm were dipped into the liquid SB102.

At least five samples were tested for each parameter. The amount of dissolved SAC305 wires was calculated by observing the differences in the cross-sectional areas before and after the immersion test, and the images were observed via an optical microscope (OM, BX51M, Olympus) after grinding and polishing.

The shear test samples were fabricated by assembling a die on both the hybrid solder joint and SB102. The mechanical properties were determined using the shear test equipment (DAGE 4000PXY) with a shear height around the mid-height of the die, and the shear speed was set as 50 µm/s. The shear height was determined from the bottom side of the PCB to the center of the capacitor. The shear height was around 300 µm. The direction is perpendicular to the long side of the capacitor. The contact areas were calculated from the Cu pads beneath the capacitors. Since all the samples were measured using the same approach, we believe that the comparison for the shear strength is reasonable.

Results and Discussion

SB102/SAC0307 Hybrid Solder Joint Microstructure After Reflow

Figure 1 shows the cross-sectional images of SB102 and the hybrid solder joint reflowed at 170°C and 190°C that were observed by SEM with a BSE mode. A clear boundary can be seen between SB102 and SAC0307; thus, the image presents a two-layered structure with SB102 on top and SAC0307 on the bottom. However, the SB102 microstructure in the hybrid solder joint is different from that of the reference sample. During the second reflow process, the temperature was set between the melting point of SB102 (~139°C) and SAC0307 (~218°C). The reflow profiles yielded a liquid/solid interdiffusion reaction during the reflow. The liquid SB102 on top continuously dissolved Sn from the solid SAC0307. For solid SAC0307 on the bottom, Bi continuously diffused into β -Sn grains, forming a solid solution. From the Sn–Bi phase diagram, eutectic Sn–Bi shifted to hypoeutectic during reflow and underwent a non-equilibrium cooling. The SB102 microstructure in the hybrid solder joint was expected as eutectic formed within the β -Sn dendritic matrix.

Kinetic Analysis of SB102/SAC305 Liquid/Solid Interdiffusion

To kinetically understand the dissolution of Sn from the SAC solder into molten SB102, an SAC305 wire was placed in the molten SB102 bath. SAC305 replaced SAC0307 due to its availability. Owing to the similar composition, the study on the SB102/SAC305 system should

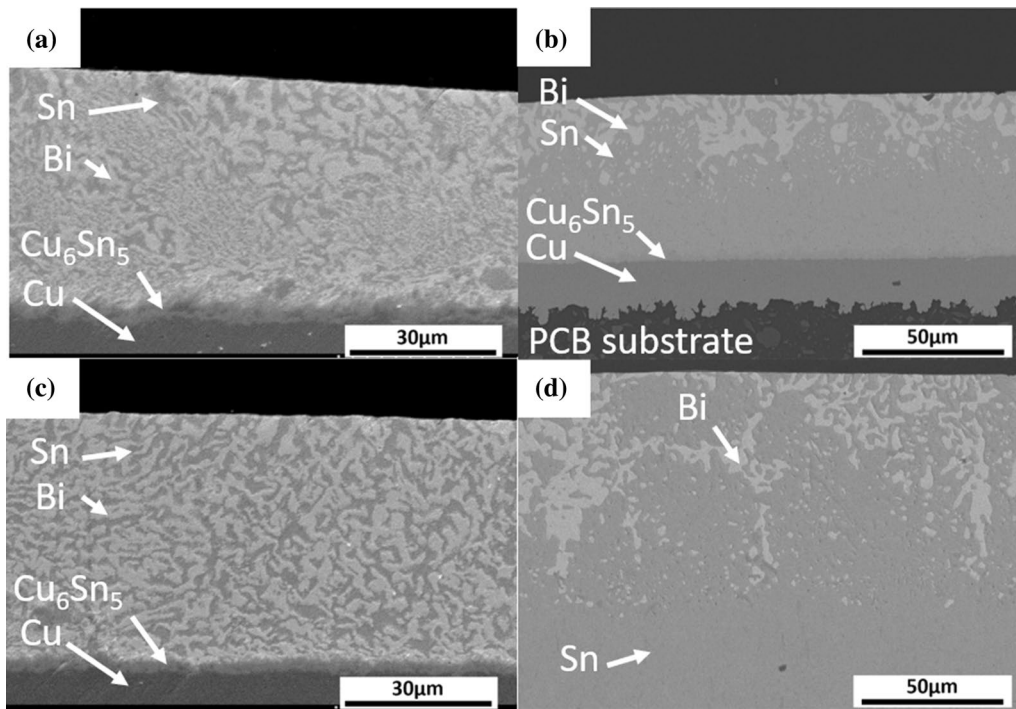


Fig. 1 Microstructure of (a) SB102 reflowed at 170°C, (b) hybrid solder reflowed at 170°C, (c) SB102 reflowed at 190°C, and (d) hybrid solder reflowed at 190°C.

help in understanding the reactions between SB102 and SAC0307. The temperature was set at 140°C, 150°C, and 160°C for different reaction durations. After the reaction, the area of the remaining SAC wire decreased with increasing reaction time. By comparing the SAC wire areas before and after the reaction, an empirical power function could be employed to analyze the dissolution rate of the Sn wire during the reaction. The corresponding equation can be written as:

$$(r_0 - r) = kt^n \quad (1)$$

In Eq. 1, r_0 is the initial radius of the SAC305 wire, r is the radius of the remaining wire, t is the reaction time, k is the dissolution rate of Sn, and n is a time exponent. The wire is assumed to have a circular shape; thus, its radius can be calculated based on the measurement of the remaining areas of residual SAC305 wire. Hence, $(r_0 - r)$ is the amount of the consumed SAC305 wire. Figure 2 shows the consumed radius of the SAC305 wire with respect to reaction time. Evidently, the consumed radius increases with the elevated reaction temperature for the same reaction time. Furthermore, the logarithm (log) of Eq. 1 yields Eq. 2 as shown below.

$$\ln(r_0 - r) = \ln k + n \ln t \quad (2)$$

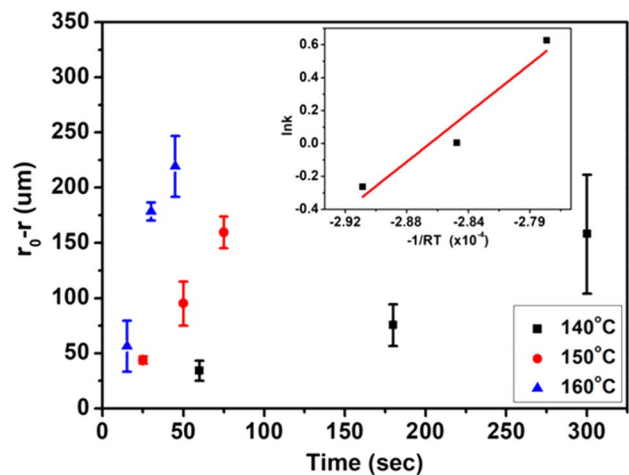


Fig. 2 Consumed radius vs. reaction time at three temperatures: 140°C, 150°C, and 160°C (inset) Apparent activation energy for Sn dissolving in liquid SB102.

The reaction constant, k , can be written as an Arrhenius equation that can be used to determine the apparent activation energy for Sn dissolving in liquid SB102 solder,

$$k = k_0 \exp \frac{(-Q)}{RT} \quad (3)$$

where k_0 is a constant, Q is the activation energy, R is the gas constant, T is the reaction temperature and the reaction constant, k , can be correlated with activation by taking natural logs on both sides of the equation. By plotting $\ln k$ with respect to $1/RT$, the slope of the line can be denoted as the activation energy Q , as shown in Fig. 2. The activation energy was deduced from the plot as 65.93 kJ/mol. This value is lower than the results previously reported in the literature.^{8–10} Possibly, the driving force in our study is the concentration gradient of Sn between SAC305 and SB102. Without the formation of the IMC layer between SAC and SB102, Sn could easily diffuse to liquid SB102.

SB102/SAC0307 Hybrid Solder Joint Long-Term Aging

Microstructure Evaluation After Thermal Aging

The evolution of the microstructure for the hybrid solder joint during the aging process was found to demonstrate the effect of the addition of the SAC0307 layer. Figure 3 shows the BSE images of SnB102/SAC0307 reflowed at 170°C and 190°C, then aged at 100°C for 15 days. As shown in Fig. 3b, small Bi particles precipitated in the β -Sn grains and were distributed uniformly in the SAC0307 solder post-aging. The same results were also observed when the hybrid solder joint was reflowed at 190°C and aged at 100°C for 15 days, as shown in Fig. 3d.

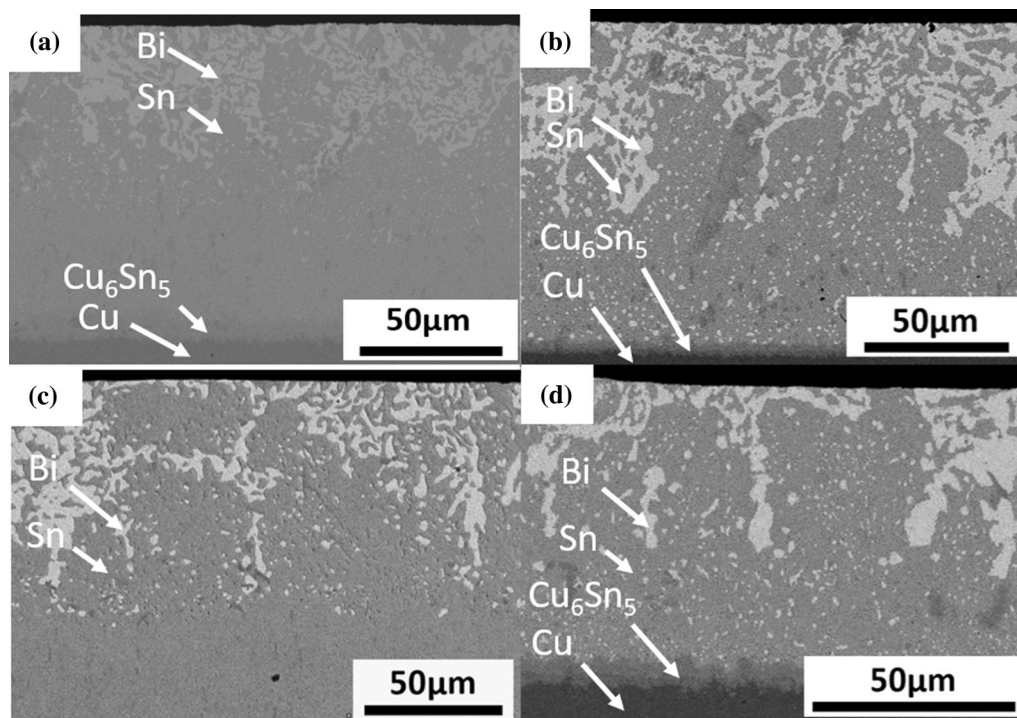


Fig. 3 Microstructure of the hybrid solder (a) as-reflowed at 170°C and aged for (b) 15 days; (c) as-reflowed at 190°C and aged for (d) 15 days.

Mechanical Properties of the Hybrid Solder Joint After Thermal Aging

To confirm the contribution of the SAC0307 layer to the mechanical properties of the solder matrix after the long-term heat treatment, the microstructure, fracture surface, failure mode, and shear strength were analyzed. Figure 4 displays a schematic drawing of the sample, where a die was assembled on a substrate with reflowed solders on the two legs. The rectangular box indicates the cross-sectional areas reflected in the images. The cross-section of the hybrid solder joint in the shear test samples reflowed at 170°C is shown in Fig. 5a. After assembling the die

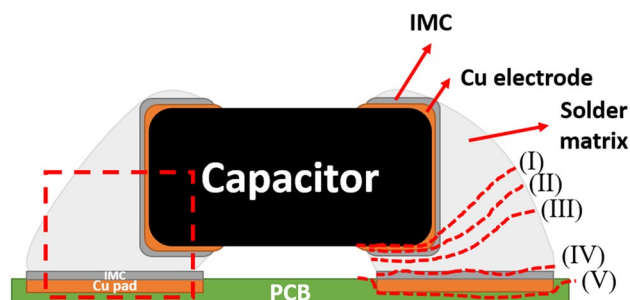


Fig. 4 Schematic figure of a shear test sample. The rectangular on the left is the area for microstructure observation. The five dotted lines on the right represent five locations of fracture: (I) Cu electrode, (II) IMC/solder, (III) Solder matrix, (IV) Solder/IMC, and (V) PCB.

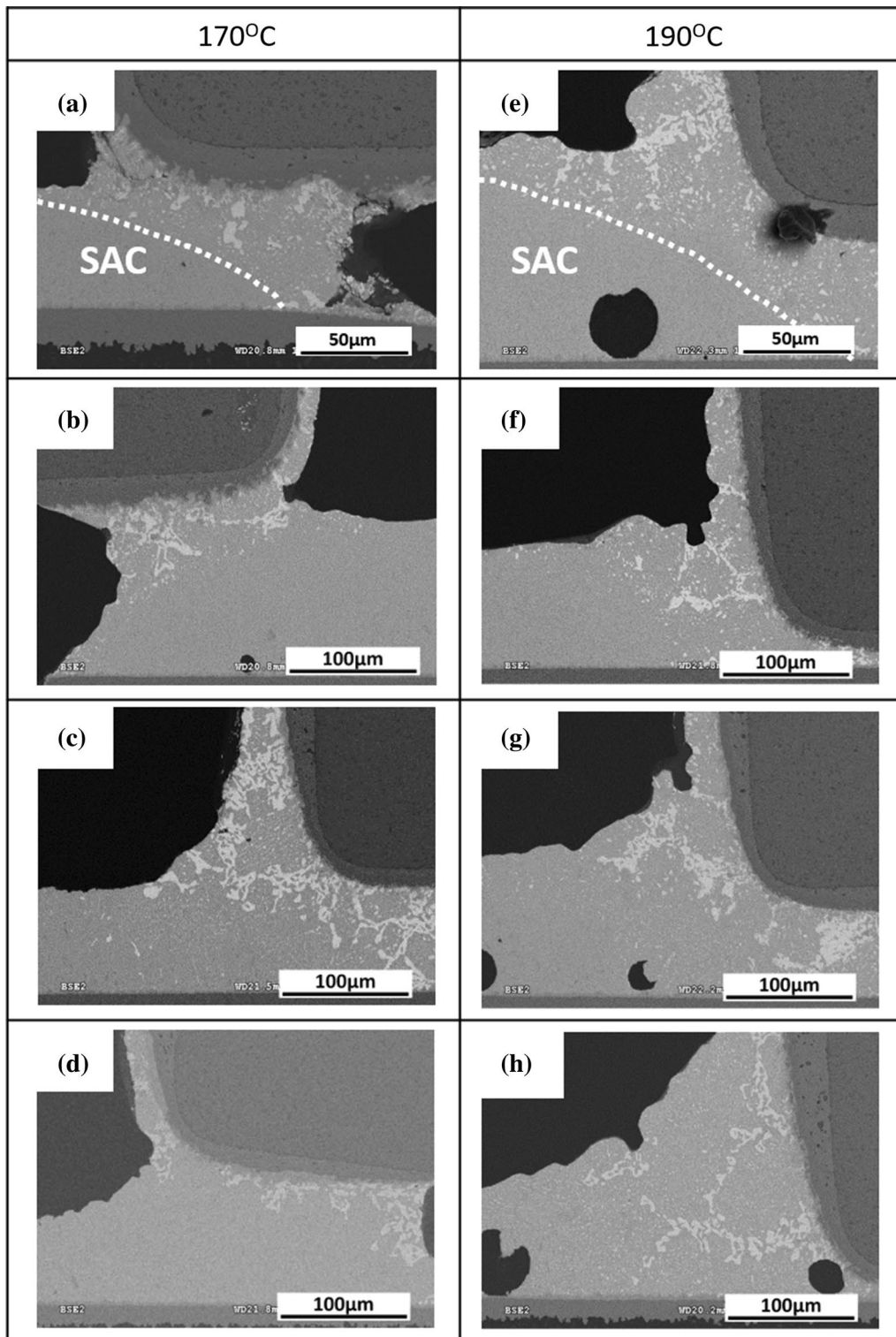


Fig. 5 Images from the rectangular box shown in Fig. 4. Microstructure of hybrid solder reflowed at 170°C (a) as-reflowed, (b) aging at 75°C for 15 days, (c) aging at 100°C for 15 days, (d) aging at 125°C

for 15 days; hybrid solder reflowed at 190°C (e) as-reflowed, (f) aging at 75°C for 15 days, (g) aging at 100°C for 15 days, (h) aging at 125°C for 15 days.

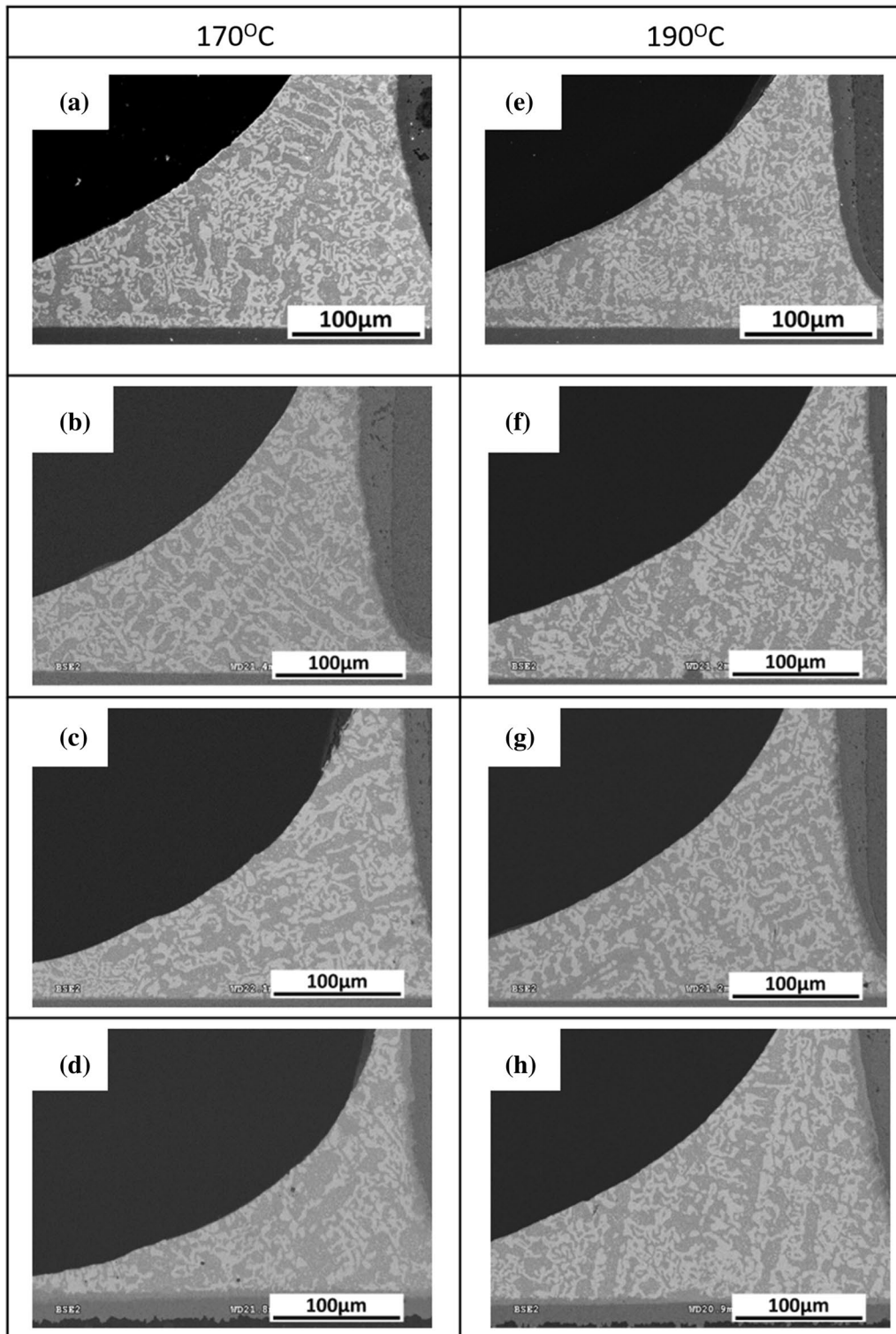


Fig. 6 Images from the rectangular box shown in Fig. 4. Microstructure of SB102 solder reflowed at 170°C (a) as-reflowed, (b) aging at 75°C for 15 days, (c) aging at 100°C for 15 days, (d) aging at 125°C

for 15 days; hybrid solder reflowed at 190°C (e) as-reflowed, (f) aging at 75°C for 15 days, (g) aging at 100°C for 15 days, (h) aging at 125°C for 15 days.

with the hybrid solder joint, the solder matrix formed a two-layer structure with SB102 on top and SAC0307 on the bottom. The hybrid solder joint microstructure after aging at 75°C, 100°C, and 125°C for 15 days is shown in Fig. 5b–d. The results show numerous small Bi particles precipitated in the β -Sn grains and distributed uniformly with aging at 100°C and 125°C. However, no Bi was observed with aging at 75°C for 15 days. Similar results were found when the hybrid solder joint was reflowed at 190°C. Small Bi particles were precipitated out of the β -Sn grains due to the exceedance of maximum solubility. SB102 was compared with the hybrid solder joint, which was also reflowed at 170°C and 190°C, followed by aging at 75°C, 100°C, and 125°C for 15 days. The cross-sectional images are shown in Fig. 6. Bi-rich phases became coarser after long-term aging. By adding minor quantities of Ag and Cu in SB102, no continuous Bi-rich phase formed at the interface between the solder matrix and the IMC layer. The fracture surface of SB102 and the hybrid solder joint after the reflow and aging at 125°C for 15 days are shown in Fig. 7. For SB102, a large brittle fracture surface could be observed in both cases. However, with the addition of the SAC0307 layer, the fracture surface transformed from brittle to a dimple morphology in the entire fracture area. The results clearly indicated that the

failure mode was successfully converted from brittle to ductile. From the fracture surface morphology, five types of failure modes could be concluded based on the fracture location. As schematically presented in Fig. 4, the fracture locations included the Cu electrode, IMC/solder, solder matrix, solder/IMC, and PCB. The failure mode percentages for SB102 and the hybrid solder joint aged at 75°C, 100°C, and 125°C for 5, 10, and 15 days are shown in Fig. 8. SB102 showed no obvious tendency when aged at 75°C and 100°C for 15 days. However, when the aging temperature reached 125°C, the dominant failure mode changed from the Cu electrode to the solder matrix or solder/IMC. The results could be attributed to the decreasing solder strength caused by the coarsening of Bi-rich phases. However, the fractured location of the hybrid solder joint changed from the solder matrix to the Cu electrode, suggesting that the solder matrix's strength was enhanced by the long-term aging process and exhibited good ductility. Wang et al. reported that Bi-segregations form near the Cu substrate accompanied by the formation of Cu_6Sn_5 IMC. The accumulation of Bi near the surface may inhibit the growth of the interfacial IMC during the subsequent aging process.¹¹ This study shows that the addition of Bi in the solder degrades the joint strength. In this study, Bi segregation is more prominent in the SB 102 than in the hybrid

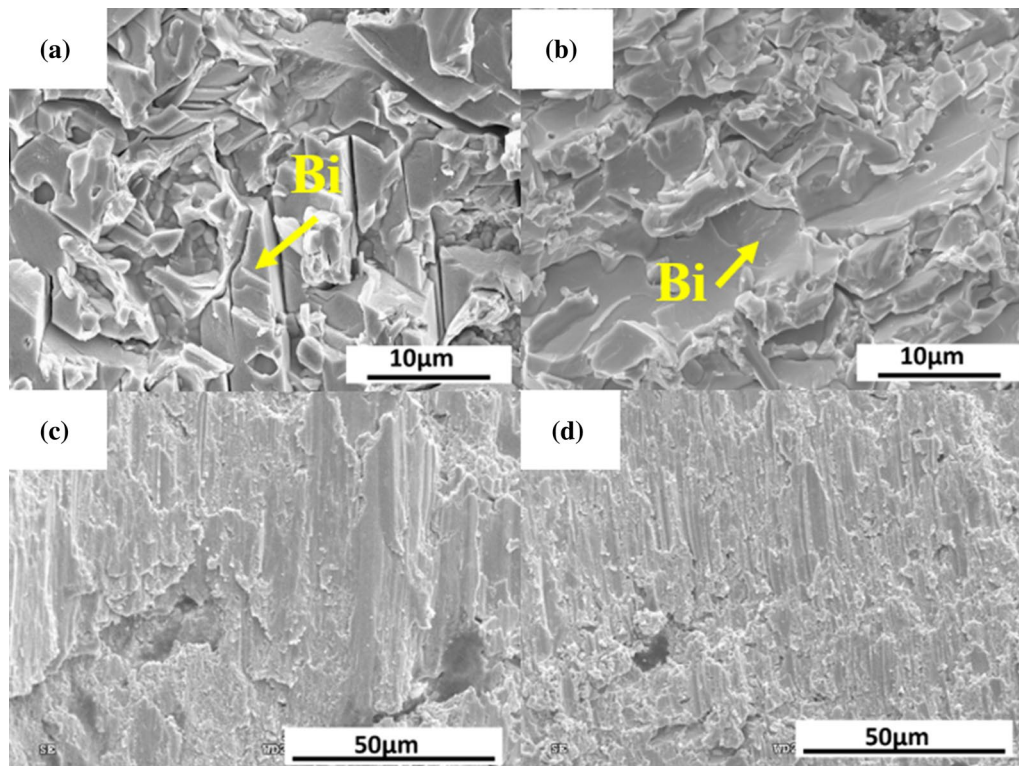


Fig. 7 Fracture surface of SB102 solder reflowed at (a) 170°C and (b) 190°C and aging at 125°C for 15 days; hybrid solder reflowed at (c) 170°C and (d) 190°C aging at 125°C for 15 days.

solder joint, as can be seen from Figs. 5 and 6. In the hybrid solder joint, the composition varies from eutectic to hypoeutectic; hence, it is expected that Bi would dissolve in the matrix and diffuse toward the SAC0307 side.

The shear strengths of SB102 and the hybrid solder joint are shown in Fig. 9. The strength of the hybrid solder joint greatly increased with both the aging time and temperature. Small Bi particles precipitated in the β -Sn grains strengthened the solder due to precipitation and solid solution strengthening. The results prove that the hybrid solder joint could endure a harsh environment exhibiting good strength and ductility. The shear height was determined from the bottom side of the PCB to the center of the capacitor. The shear height was around 300 μm . The direction is perpendicular to the long side of the capacitor. It is possible that the shear strength of the die would decrease with increasing shear height due to torque generated by the shear force. According to the test standard SEMI G63-95, there is a table that shows the corresponding values of minimum shear strength to different shear test height ratio. Therefore, the proposed

hybrid solder joint may be a very promising choice as a low-temperature assembling material.

Conclusions

The addition of the SAC layer reduced the ratio of Bi-rich phase in the SB102 matrix and changed the SB102 microstructure from eutectic to hypoeutectic via non-equilibrium cooling. The results of the liquid/solid interfacial kinetic analysis confirm that the dissolution rate of SAC increased with the reflow temperature, with activation energy of 65.93 kJ/mol. With the addition of the SAC layer between the SB102 and Cu substrate, the fracture mode changed from brittle to ductile. Small Bi particles precipitated in the β -Sn grain after the heat treatment, and the shear strength of the hybrid solder joint increased due to precipitation and solid solution strengthening.

1. The addition of the SAC layer reduced the ratio of Bi-rich phase in the SB102 matrix and changed the micro-

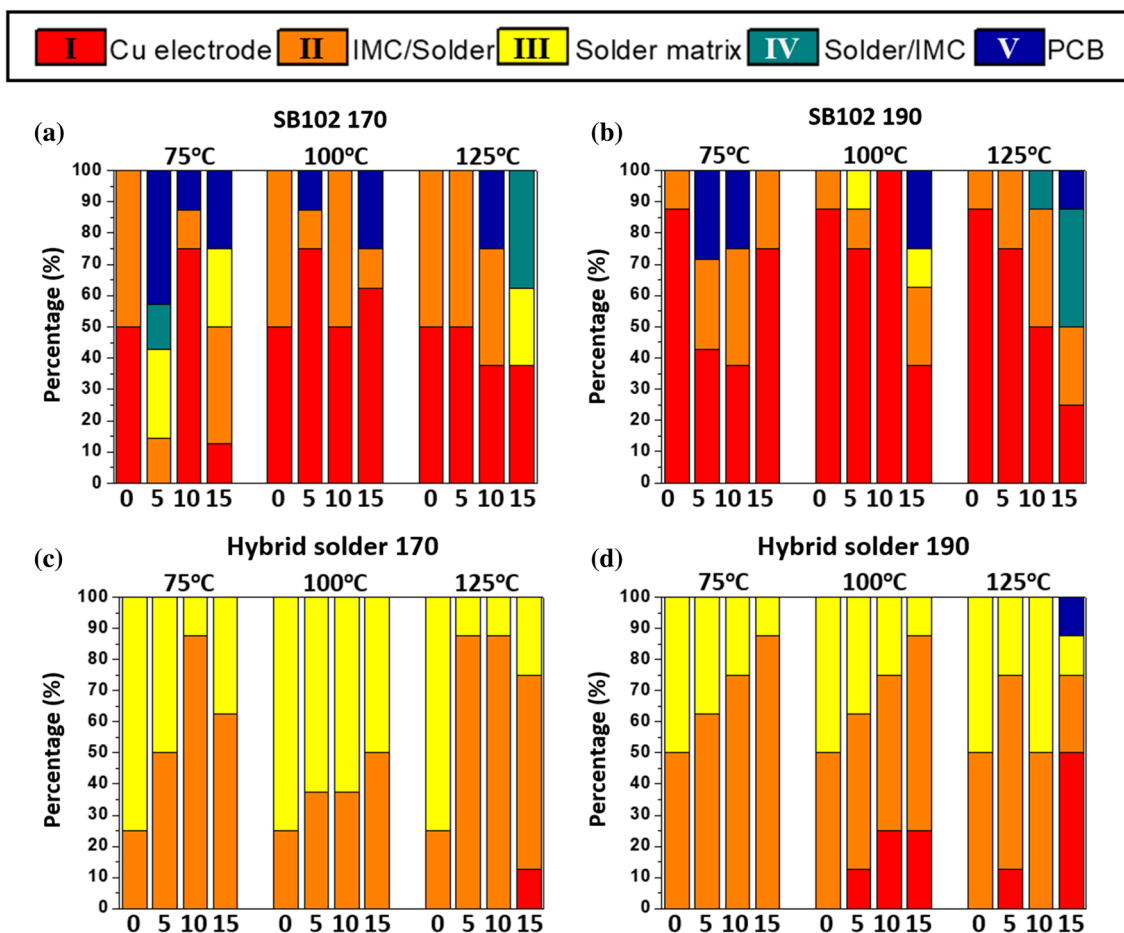


Fig. 8 Percentage of failure mode for (a) SB102 reflowed at 170°C, (b) SB102 reflowed at 190°C, (c) hybrid solder reflowed at 170°C, and (d) hybrid solder reflowed at 190°C. The data show the as-reflowed sample, the aging sample for 5, 10, and 15 days at 75, 100, and 125°C.

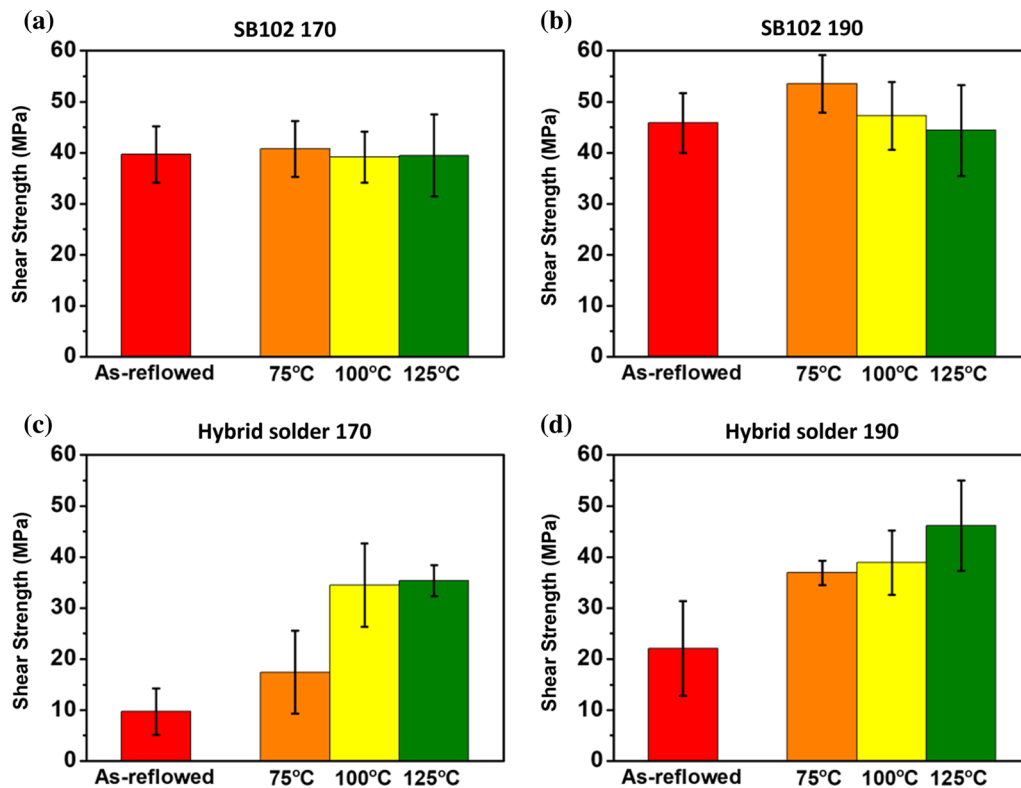


Fig. 9 Shear strength of (a) SB102 reflowed at 170°C, (b) SB102 reflowed at 190°C, (c) hybrid solder reflowed at 170°C, and (d) hybrid solder reflowed at 190 after aging at 75°C, 100°C, and 125°C for 15 days.

structure of SB102 from eutectic to hypoeutectic by non-equilibrium cooling.

- From the results of liquid/solid interfacial kinetic analysis, it is confirmed that the dissolution rate of SAC increased with reflow temperature, and the apparent activation energy was 65.93 kJ/mol.
- Adding the SAC layer between SB102 and the Cu substrate could change the fracture mode from brittle to ductile.
- Small Bi particles precipitated in the β -Sn grain after heat treatment, and the shear strength of hybrid solder increased due to precipitation and solid solution strengthening.

Conflict of interest The authors declare that they have no known competing financial interests or personal relationships that could have appeared to influence the work reported in this paper.

References

- F. Hu, Q. Zhang, J. Jiang, and Z. Song, Influences of Ag addition to Sn-58Bi solder on SnBi/Cu interfacial reaction. *Mater. Lett.* 214, 142 (2018).
- Z. Wang, Q. Zhang, Y. Chen, and Z. Song, Influences of Ag and In alloying on Sn-Bi eutectic solder and SnBi/Cu solder joints. *J. Mater. Sci. Mater.* 30, 18524 (2019).
- A.K. Gain, and L. Zhang, Effect of Ag nanoparticles on microstructure, damping property and hardness of low melting point eutectic tin–bismuth solder. *J. Mater. Sci. Mater.* 28, 15718 (2017).
- J. Yang, Q. Zhang, and Z. Song, Influences of Ag and in alloying on microstructure and mechanical properties of Sn-58Bi solder. *J. Electron. Mater.* 50, 283 (2021).
- L. Zhang, and K.-N. Tu, Structure and properties of lead-free solders bearing micro and nano particles. *Mater. Sci. Eng. R Rep.* 82, 1 (2014).
- Y. Chen, Z.-C. Meng, L.-Y. Gao, and Z.-Q. Liu, Effect of Bi addition on the shear strength and failure mechanism of low-Ag lead-free solder joints. *J. Mater. Sci. Mater.* 32, 2172 (2021).
- S.W. Jeong, J.H. Kim, and H.M. Lee, Effect of cooling rate on growth of the intermetallic compound and fracture mode of near-eutectic Sn-Ag-Cu/Cu pad: before and after aging. *J. Electron. Mater.* 33, 1530 (2004).
- J.-Y. Wang, Y.-X. Lin, C.-Y. Yeh, C.-Y. Chiu, E.-J. Lin, C.-Y. Wu, C.-H. Lee, P.-J. Chang, and C.-Y. Liu, Effect of Ag solutes on the solid-state Cu dissolution in the Sn3.5Ag. *J. Mater. Sci. Mater.* 32, 567 (2021).
- A. Sharif and Y. Chan, Dissolution kinetics of BGA Sn–Pb and Sn–Ag solders with Cu substrates during reflow. *Mater. Sci. Eng. B* 106, 126 (2004).
- Y.-C. Huang, S.-W. Chen, W. Gierlotka, C.-H. Chang, and J.-C. Wu, Dissolution and interfacial reactions of Fe in molten Sn-Cu and Sn-Pb solders. *J. Mater. Res.* 22, 2924 (2007).

11. F. Wang, Y. Huang, Z. Zhang, and C. Yan, Interfacial reaction and mechanical properties of Sn-Bi solder joints. *Materials* 10, 920 (2017).

Publisher's Note Springer Nature remains neutral with regard to jurisdictional claims in published maps and institutional affiliations.

Springer Nature or its licensor (e.g. a society or other partner) holds exclusive rights to this article under a publishing agreement with the author(s) or other rightsholder(s); author self-archiving of the accepted manuscript version of this article is solely governed by the terms of such publishing agreement and applicable law.